Proceedings of the ASME 2012 11th Biennial Conference on Engineering Systems Design and Analysis
ESDA2012
July 2-4, 2012, Nantes, France

ESDA2012-82673

OPTIMIZED CONTROL STRATEGY BASED ON THE DRIVING CYCLE TYPE FOR A HYDRAULIC HYBRID BUS

Ali Safaei
M.S student
School of Mechanical Engineering,
College of Engineering, University of Tehran
Tehran, Iran
ali.safaie@ut.ac.ir

Vahid Esfahanian
Prof. of Mechanical Engineering
School of Mechanical Engineering,
College of Engineering, University of Tehran
Tehran, Iran

Mohammad Reza Ha'iri-Yazdi
Assoc. Prof. of Mechanical Engineering
School of Mechanical Engineering,
College of Engineering, University of Tehran
Tehran, Iran

Mohsen Esfahanian
Ass. Prof. of Mechanical Engineering
Dep. of Mech. Eng., Isfahan University of Technology
Isfahan, Iran

Masood Masih Tehrani
Ph.D student in Mechanical Engineering
School of Mechanical Engineering,
College of Engineering, University of Tehran
Tehran, Iran

Hassan Nehzati
M.S. student in Mechanical Engineering
School of Mechanical Engineering,
College of Engineering, University of Tehran
Tehran, Iran

ABSTRACT

Using hybrid powertrains is an attractive idea to reduce the fuel consumption in vehicles. Control strategy is the most challenging subject in designing of a hybrid powertrain. In this paper, an optimized control strategy based on the driving cycle type designed for a hydraulic hybrid bus has been presented. Because of considering the type of the driving cycle, the proposed control strategy can be named as an intelligent one. In this controller, at first, four standard driving cycles have been defined as the reference clusters. Then the optimized control strategy for each cluster has been derived using a dynamic programming algorithm. In addition, several multi-layered perceptron networks are modeled in order to use the output of each optimized control strategy. After that a clustering method with a feature selection algorithm has been implemented to assign degree of similarity to each cluster for the unknown driving cycle. Finally, a linear combination of four optimized control strategy outputs has been used for generating final output of the intelligent control strategy. In this combination, each output is weighted by the corresponding degree of similarity. Here, the hydraulic hybrid bus model is a feed forward one and has been simulated using a compound driving cycle. The compound driving cycle consists of six distinct 100s long portions of the Nuremburg driving cycle. The simulation results show that by using the intelligent control strategy, the fuel consumption of the hybrid bus has been reduced by almost 12% in comparison with the results of a rule-based control strategy.

INTRODUCTION

A parallel hydraulic hybrid (PHH) powertrain, using a combination of an Internal Combustion Engine (ICE) and a hydraulic Pump/Motor (P/M) is an important concept to improve fuel economy and to reduce emission of vehicles as well. This technology has more power density and also lower energy density than electric hybrids. According to these special characteristics, hydraulic hybrid technology is mostly used in large vehicles like trucks and buses as their potential for regenerative braking is higher than passenger cars.

Designing and implementation of a hybrid powertrain presents some challenging problems. In particular, distribution of vehicle demand torque between two power sources is the most important subject. This torque distribution is performed through a control strategy. In 2007, Salmasi [1] classified all control strategies for hybrid powertrains in two main groups, including control strategies based on driving cycle type. The first group includes those which are named as rule-based control strategies. These control strategies are based on some rules that are generated by experts. The rules could be in non-fuzzy scheme or fuzzy scheme. Usually rule-based control strategies are far from optimum strategy. The second group are those that extracted by using an optimization algorithm. Dynamic programming (DP) is the most popular algorithm for performing optimized control strategy in hybrid powertrains. The problem of these control strategies is that they would be the optimum choices only for one special driving cycle. One can define a separate group for such these control strategies. Control strategies based on driving cycle type consider the environmental conditions of the vehicle and are named as intelligent control strategies. The types of driving cycle, level of congestion on the road and the number of stop/start of vehicle in the driving cycle are examples for environmental conditions. Won and Langari [2, 3] presents an intelligent control strategy for an electric hybrid car in 2003. They generated fuzzy rule-based torque distributer for each of 9 standard driving cycles. Then a driving pattern recognition process has been performed for an unknown driving cycle and a control strategy is chosen among the extracted strategies. This phase has been performed according to the similarity of every portion of driving cycle to one of the standard driving cycles. In 2007 A. Abdollahi [4], did the similar work. She extracted an optimal control strategy for every standard driving cycle using a static optimization algorithm. Then rules of fuzzy rule-based control strategy were generated using the results of optimization algorithm. Also the number of features used for recognition of an unknown driving cycle has been reduced to 5 respects to those in Won's work which was 16 features. In two above works a Linear Vector Quantization (LVQ) network have been used for driving pattern. J. Park et.al [5], in 2009 developed a multi-layered multiclass neural network for driving pattern recognition. Then a special function has been suggested for representing the fuel rate of ICE in an electric hybrid powertrain according to the type of the road. Finally a quadratic programming was used to determine the optimal torque distribution respect to the recognized function for fuel rate. In 2010 X. Huang et.al [6], used four features for discriminating between the driving cycle types. He considered only 2 driving cycle types. In addition, two non-fuzzy rule-based control strategies have been developed for each of driving cycle types. Finally the control strategy for a hybrid powertrain in an unknown driving cycle has been extracted according to the driving cycle type.

In all the above works, every portion of a driving cycle was assigned to only one standard driving cycle type. It is better to assign some weights for similarity of an unknown driving cycle to the standard ones. In other words, one cannot say that a driving cycle is exactly (100%) similar to one standard driving cycle; instead one should say the similarities of a driving cycle to each standard driving cycle type through some weights. This idea is developed in this work using a fuzzy clustering method. Fuzzy weights represent the similarity of every unknown driving cycle to each of standard ones. In addition, the feature selection is performed by a floating search method, which is flexible to reconsider the features previously discarded and also discard features previously selected [7]. Using a DP method, the optimal decisions in every situation for 4 standard driving cycles have been generated. Extraction of optimal decision for every input has been performed using a multi-layered perceptron (MLP) network. After that regarding the fuzzy weights for an unknown driving cycle, a linear combination of optimal results for each standard driving cycle is used to generate the torque distribution in hybrid powertrain. In this study the intelligent control strategy is implemented on the model of a hydraulic hybrid bus. The model is a feed forward one and is generated in MATLAB/Simulink.

FEED FORWARD MODEL OF HYDRAULIC HYBRID BUS

As mentioned earlier, the configuration of the hybrid powertrain in this paper is a parallel hydraulic one. A schematic for the hybrid powertrain can be seen in Fig. 1. The parallel hydraulic hybrid bus contains four major components in its powertrain. These are the ICE, hydraulic P/M, the bladder type accumulators and the transmission. Also the transmission includes an automatic gearbox with 4 forward gears and 1 rear gear, a one speed gearbox and a post-transmission torque coupling. The automatic gearbox is used to modify the ICE output torque and the one speed gearbox does the same for the hydraulic P/M.

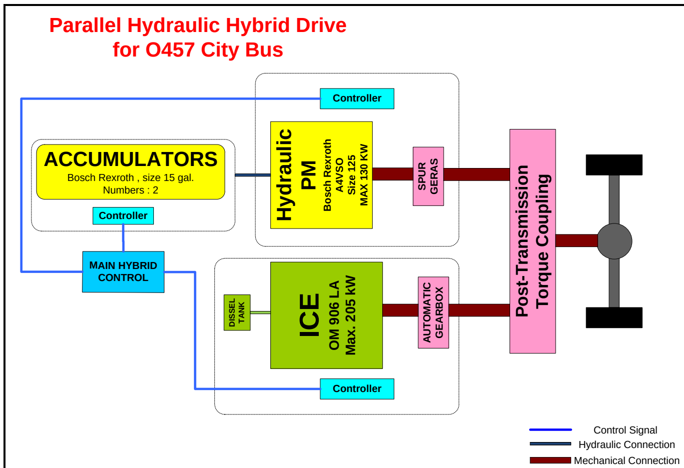

Figure 1- The schematic diagram of PHH powertrain

The specifications of the major components have been chosen by considering the designing procedure explained in [12]. The designing procedure considers the performance requirements of an urban bus. The general specifications of entire bus and also powertrain components are presented in Table 1.

Table 1. The specification of parallel hydraulic hybrid bus

Gross Weight	9820(kg)
Weight considering the passengers	14720(kg)
ICE	**OM906LA** Max power : 205 kW Max torque : 1100 Nm
Hydraulic P/M	**A4VSO** Max power : 131 kW Max torque : 696 Nm Maximum displacement : 125 cc/rev
Gearbox	Automatic transmission with 4 speeds
Accumulators	2 bladder type Maximum operating pressure : 345 bar Nominal Volume : 50 liters (each one)

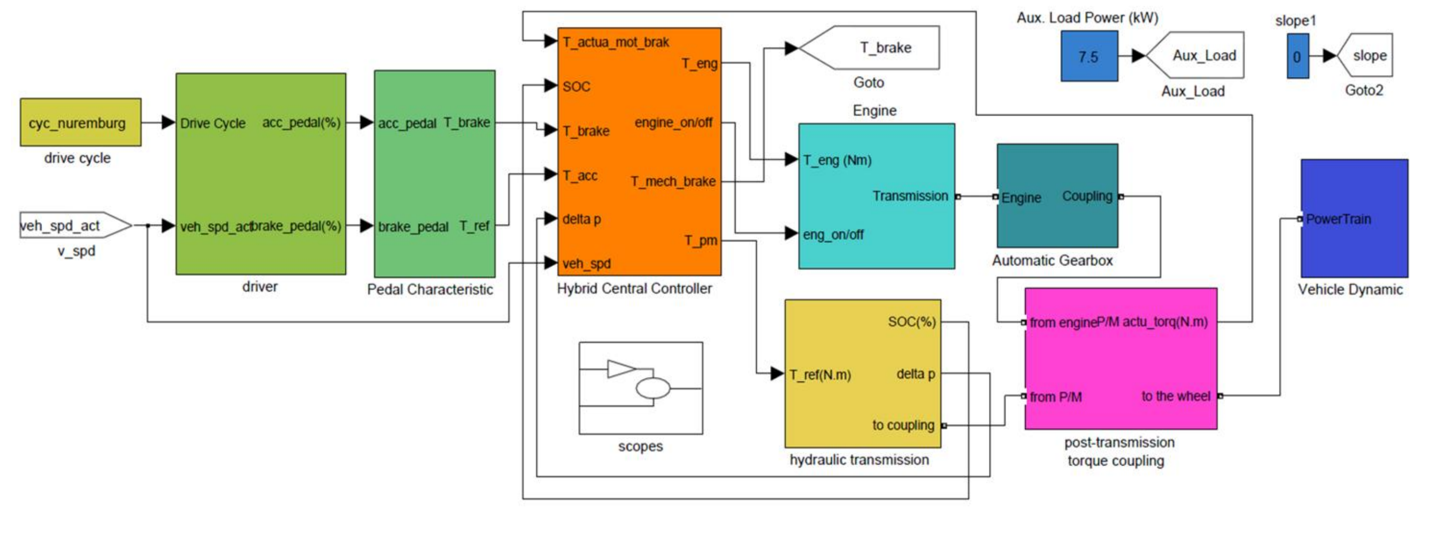

Figure 2 – The entire model of PHH bus in Simulink

According to the hybrid powertrain presented above, the model of PHH bus has been generated in MATLAB/Simulink using the SimScape blocks. The entire bus model consists of several blocks corresponding to each component. The modeling has been done considering the efficiency of each component. The values for the efficiency of each component have been extracted from their corresponding catalogues. Arrangement of the blocks in the PHH bus model can be seen in Fig. 2. In this feed forward model, the driver block creates appropriate command signal according to the difference between the driving cycle speed and the actual vehicle speed. This signal is sent to the Hybrid Central Control (HCC) block. The HCC block is the heart of the hybrid model and computes the torques of each power sources so as to satisfy the driver demand. The performance of this block is based on the designed control strategy. The output signals of the HCC block is sent to the ICE and hydraulic P/M blocks. These two blocks generate the demanding torques. Finally, both output torques are coupled in the torque coupling and the final signal is sent to the vehicle dynamic block. The equations for dynamics of bus considering the resistance forces are modeled in the vehicle dynamic block.

In the PHH bus model, the fuel consumption of the bus is computed in ICE block considering the BSFC[1] map of the engine. Also, the hydraulic transmission block contains both the hydraulic P/M model and also the accumulator model.

Three subsystems have been considered in order to model the hydraulic P/M. One of them is for computing the efficiency of P/M for different values of its torque and speed. As mentioned before, the efficiency values have been gathered using an efficiency map in the P/M catalogue. The other subsystem is for generating the output torque of hydraulic machine in both pump mode and motor mode operations. Also the third subsystem controls the output torque of the hydraulic the hydraulic P/M and actual output torque signal of the P/M. In practice this controller is a hydro-electrical control circuit which operates on the value of the swash-plate angle. It should be noted that the hydraulic machine used in this paper is an axial piston machine with variable displacement. The model of the hydraulic P/M has been shown in Fig. 3.

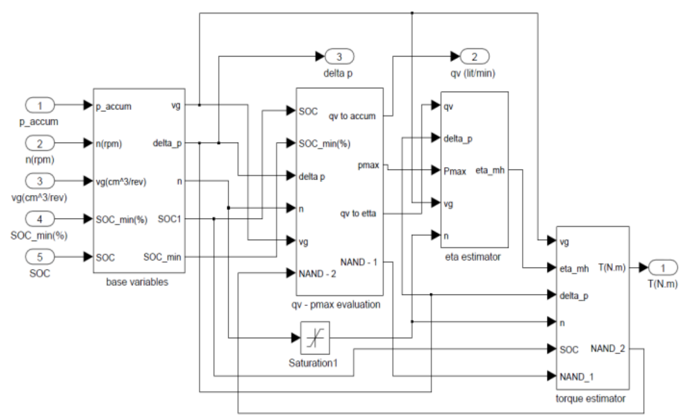

Figure 3 – Model of hydraulic pump/motor

The accumulators used in the PHH bus model are of the bladder type. The bladder type accumulators consist of two sides. One of them is for the hydraulic fluid and there is an inert gas (N_2 used in many accumulators) in the other side. These two sides are separated by a diaphragm. In order to model the bladder accumulators, the thermodynamic process which N_2 gas acts on was considered as an adiabatic one. By this consideration, the values of the hydraulic fluid that can be stored in the accumulator at each pressure difference can be computed using a map from the catalogue. The efficiency of accumulator operation has been considered in this map. Also

[1] Brake Specific Fuel Consumption

the state of charge (SOC) for the accumulators' package has been evaluated using the following formula

$$SoC(\%) = \frac{v_x}{v\_\max} \times 100 \tag{1}$$

in which the v_x is the current volume of the stored fluid and *v_max* is the maximum fluid which can be stored in the accumulators.

Finally, it should be noted that the control strategy for managing the torques of the two power sources would be implemented in HCC block. The complete procedure of the PHH bus modeling has been explained in [12].

OPTIMIZED CONTROL STRATEGY FOR STANDARD DRIVING CYCLES USING DYNAMIC PROGRAMMING

The control strategy for torque management in the proposed PHH bus is a linear combination of four optimal control strategies. These control strategies are optimized for four standard driving cycles. The standard driving cycles (Fig. 4) are adopted from those which are developed in Sierra Research Inc. [8]. They have been selected according to the popular driving cycle of an urban bus; that is not a freeway driving cycle.

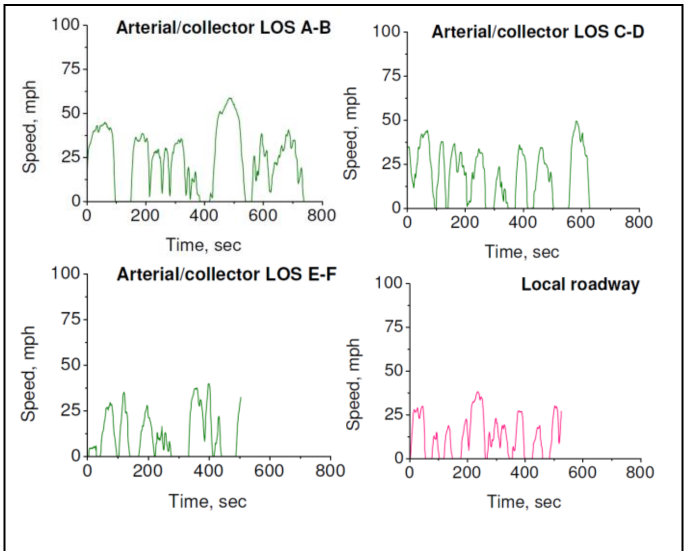

Figure 4 – Four standard driving cycle

According to the dynamic nature of the hybrid powertrain model, DP would be a profitable optimization algorithm. Optimized control strategy for four standard driving cycles has been evaluated using a discrete DP algorithm [9, 10]. Inputs for the algorithm are the driver demand torque, vehicle speed and the gear number in the automatic gearbox of the PHH bus model. The gear number shifting in the automatic gearbox is a function of vehicle speed. So we did not consider the gear number as a control parameter; instead the gear number in each step time used as an input parameter. The inputs have been logged in 1 second. In addition, the SOC of accumulator is considered as state variable. In order to perform discrete DP algorithm, the space of SOC as the state variable should be quantized. The value of quantization step is 0.001. This value would limit the minimum step in space of P/M generated torque. The lower is the SOC quantization step, the lower is the P/M torque step. Also the least value of the SOC step is regulated by the specification of RAM and CPU of processing computer. The value of 0.001 was profitable regarding the two above limitations. Using the input variables, the presented DP algorithms progressed in the following way:

at first, the upper and lower band of SOC has been determined considering the maximum and minimum torque of P/M. After that in forward direction, the optimum state in *i*th step time has been evaluated for each SOC node in (*i+1)*th step time (Fig. 5 [10]). This procedure was continued through the whole duration of time for a given driving cycle. Finally, considering the equality of initial and final SOC, the optimum state at each step time has been specified in backward direction.

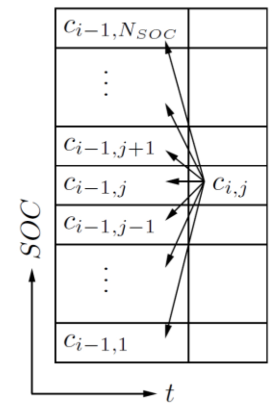

Figure 5 – Forward direction of DP algorithm in each step time

The output of DP algorithm is the optimal direction for the SOC of accumulator over the whole driving cycle in order to level initial and final SOC. Also the required output torques of ICE and P/M in each step time has been generated. The constraints on the optimal control problem are:

$$\begin{gathered} 0.2 < SOC < 0.9 \\ 0 < T\_eng < T\_eng\_max \\ T\_pm\_min < T\_pm < T\_pm\_max. \end{gathered} \tag{2}$$

The boundaries of SOC are defined considering the safety of accumulators. Also the boundaries for ICE and P/M torques are gained from their corresponding performance diagrams. Ideally, the torque distribution has to be chosen to minimize the overall engine fuel consumption over a given driving cycle within the constraints listed above, such as:

$$Min \sum m_f(t) \tag{3}$$

where $m_f^{\cdot}(t)$ is the fuel rate of ICE in each step time.

The optimal path of the SOC in one of the standard driving cycles derived from proposed discrete DP algorithm is shown in Fig. 6. As can be seen the initial and the final SOC of the accumulators are equal. Also the changes of the SOC are in the way to keep the maximum available fluid volume in the accumulators. In addition, the optimal torques for ICE and P/M are presented in a short period of time for this standard driving cycle in Fig. 6. It is interesting to see how the ICE and hydraulic P/M satisfy the driver demand torque. Also, it should be noticed that the mechanical brakes supply the excessive torque to hydraulic P/M torque when the bus is in braking situations.

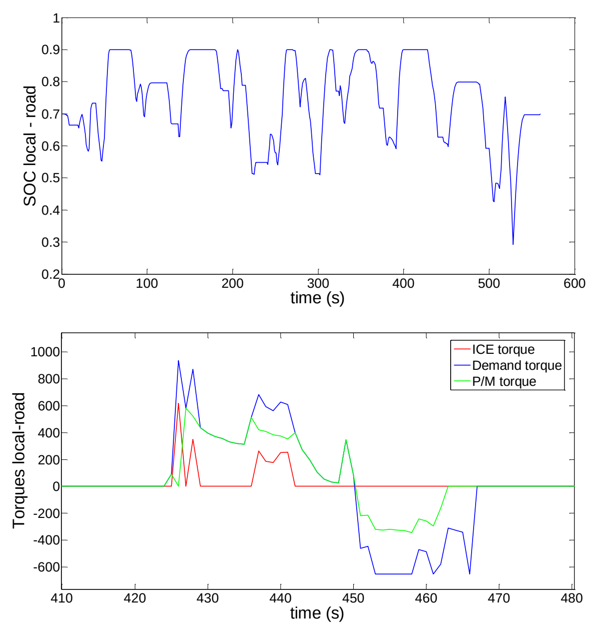

Figure 6 – Optimal SOC path and optimal torques of ICE and P/M (in a short period of time) for local roadway driving cycle

After extraction of optimal values for the ICE torque at each step time, a model should be generated to use these values. So, some MLP networks have been generated using NNtool toolbox in MATLAB. According to very strong nonlinear behavior of the DP algorithm results, every portion of data has been modeled by a specific network. For each standard driving cycle, the DP results divided to 4 or 5 groups regarding the SOC values. After that a MLP with two layers and specific number of neurons has been modeled for each of these groups. For example, for the SOC value between 0.6-0.7 and also between 0.8-0.9, two different MLP networks have been generated. Numbers of neurons are defined by checking all possible choices to reach the least value for mean squared error of validation data. The procedure of generating the MLP networks' outputs has been shown in Fig. 7.

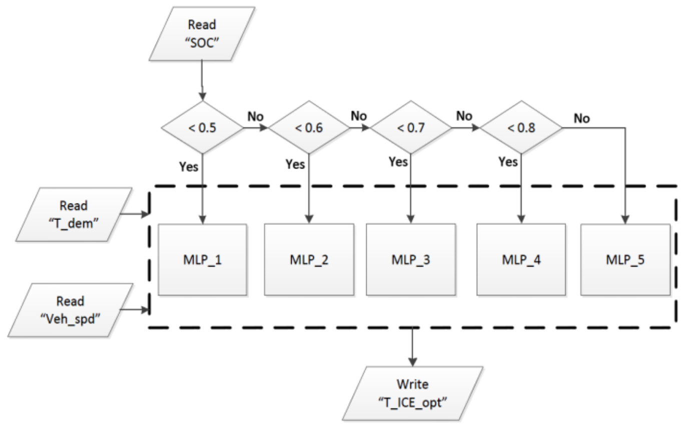

Figure 7 – Procedure of generating the MLP networks' output for each of the DP algorithms

In the MLP networks, the driver demanding torque and the vehicle speed are the inputs and the output is the optimal ICE torque. All inputs and output values are normalized. The outputs of MLP networks generated here would be used in the simulation of the hydraulic hybrid bus model.

FEATURE SELECTION AND FUZZY CLUSTERING

Every driving cycle can be recognized through some driving features. Ericson [11] defined 69 driving features for a given driving cycle. Won and others who worked on driving features have stated that all of these features are not useful in driving pattern recognition. So a feature selection process should be organized to select useful features and eliminate others. Lists of all features that are considered as the reference set in this study are presented in Table 2. These are chosen according to the former works [3-6]. Ericson presented the intervals for speed, acceleration and deceleration regarding the characteristics of a passenger car. In Table 2, the intervals have been updated according to the driving characteristics of an urban bus. Also in this table, Positive Kinetic Energy (PKE) is derived by

$$PKE = \frac{\sum(v_f^2 - v_s^2)}{x} \quad , \quad \text{when } \frac{dv}{dt} > 0 \tag{4}$$

and the Relative Positive Acceleration (RPA) is determined by following equation

$$RPA = \frac{1}{x} \times \int va^+ dt \tag{5}$$

In two above formulas, x is distance of the cycle, v is the speed and a^+ is the acceleration of the bus.

Here a method known as floating search method [7] has been used as feature selection algorithm. In this method we start with one arbitrary feature and then continue by adding the best feature which causes to reach the minimum clustering error. Also in every step the least sufficient feature is removed. The process is continued until all features are considered. The final results of floating search method are the best combination for every possible number of features.

Table 2. Reference set of driving features

Num	Feature	Num	Feature
1	Average speed (km/h)	18	Average deceleration (m/s2)
2	Maximum Speed (km/h)	19	Maximum Deceleration (m/s2)
3	% of time speed is between 0-10 km/h	20	% of time Deceleration is between 0,-0.2 m/s2
4	% of time speed is between 10-20 km/h	21	% of time Deceleration is between -0.2 , -0.4 m/s2
5	% of time speed is between 20-30 km/h	22	% of time Deceleration is between -0.4 , -0.6 m/s2
6	% of time speed is between 30-40 km/h	23	% of time Deceleration is between -0.6 , -0.8 m/s2
7	% of time speed is between 40-50 km/h	24	% of time Deceleration is between -0.8 , -1 m/s2
8	% of time speed is above 50 km/h	25	% of time deceleration is under -1 m/s2
9	Average Acceleration (m/s2)	26	Positive Kinetic Energy (PKE) m/s2
10	Maximum Acceleration (m/s2)	27	Number of stops per km
11	% of time acceleration is between 0-0.2 m/s2	28	Number of stops
12	% of time acceleration is between 0.2-0.4 m/s2	29	% of time production of speed and acceleration is between 0-5 m2/s3
13	% of time acceleration is between 0.4-0.6 m/s2	30	% of time production of speed and acceleration is between 5-10 m2/s3
14	% of time acceleration is between 0.6-0.8 m/s2	31	% of time production of speed and acceleration is above 10 m2/s3
15	% of time acceleration is between 0.8-1 m/s2	32	% of time production of speed and deceleration is between 0, -5 m2/s3
16	% of time acceleration is above 1 m/s2	33	% of time production of speed and deceleration is between -5 , -10 m2/s3
17	Relative Positive Acceleration (RPA) m/s2	34	% of time production of speed and deceleration is under -10 m2/s3

The results in the feature selection are checked by computing the clustering cost function. The floating search method is not supervised but can reach acceptable results. In addition, the method does not have any special complexity. The floating search algorithm is presented in Fig. 8 [7]. In this algorithm X_k contains the best combination of the k features and y_{m-k} is the set of m-k remaining features. Also $C(\{X_k, y\})$ is the cost function of the used clustering method.

As mentioned before, we have used a fuzzy clustering to represent the similarity of every unknown driving cycle to each standard one. Fuzzy c-means [7] is the implemented clustering method. The features of the each standard driving cycle have been used to define the center of four clusters (corresponding to the four standard driving cycles). After that the above feature selection method has performed for an unknown driving cycle.

- *Step I: Inclusion*
  $x_{k+1} = arg\max_{y \in Y_{m-k}} C(\{X_k, y\})$; that is, choose that element from Y_{m-k} which, combined with X_k, results to the best value of C.
  $X_{k+1} = \{X_k, x_{k+1}\}$
- *Step II: Test*
  1. $x_r = arg\max_{y \in X_{k+1}} C(X_{k+1} - \{y\})$; that is, find the feature that has the least effect on the cost when it is removed from X_{k+1}.
  2. If $r = k+1$, change $k = k+1$ and go to step I.
  3. If $r \neq k+1$ AND $C(X_{k+1} - \{x_r\}) < C(X_k)$ go to step I; that is, if removal of x_r does not improve upon the cost of the previously selected best group of k, no further backward search is performed.
  4. If $k = 2$ put $X_k = X_{k+1} - \{x_r\}$ and $C(X_k) = C(X_{k+1} - \{x_r\})$; go to step I.
- *Step III: Exclusion*
  1. $X'_k = X_{k+1} - \{x_r\}$; that is, remove x_r.
  2. $x_s = arg\max_{y \in X'_k} C(X'_k - \{y\})$; that is, find the least significant feature in the new set.
  3. If $C(X'_k - \{x_s\}) < C(X_{k-1})$ then $X_k = X'_k$ and go to step I; no further backward search is performed.
  4. Put $X'_{k-1} = X'_k - \{x_s\}$ and $k = k-1$.
  5. If $k = 2$ put $X_k = X'_k$ and $C(X_k) = C(X'_k)$ and go to step I.
  6. Go to step III.1.

Figure 8 – The algorithm of floating search method as a feature selection procedure

The value of clustering cost function has been computed in each step. The cost function is specified by

$$J_q = \sum_{i=1}^{N} \sum_{j=1}^{m} u_{ij}^{q} . d(x_i, \theta_j) \qquad (6)$$

In the above formula u_{ij} is the fuzzy weight for similarity of x_i driving cycle to θ_j cluster and $d(x_i, \theta_j)$ is the dissimilarity between them. Parameter q is the clustering factor and is a real number greater than one. Here q equals to 2. Also the dissimilarity $d(x_i, \theta_j)$ is computed by

$$d(x_i, \theta_j) = (x_i - \theta_j)^T . (x_i - \theta_j) \qquad (7)$$

According to the fuzzy c-means algorithm, the values of fuzzy weights for each of the clusters are computed. These weights are updated in every step of feature selection process, by ([7])

$$u_j = \frac{1}{\sum_{k=1}^{m} \left(\frac{d(x, \theta_j)}{d(x, \theta_k)} \right)^{\frac{1}{q-1}}} \qquad (8)$$

in which, m equals to the number of clusters (i.e. four). Also j corresponds to the each of the standard driving cycles (clusters).

STRUCTURE OF THE INTELLIGENT CONTROL STRATEGY

Structure of the intelligent control strategy can be shown as in Fig. 9.

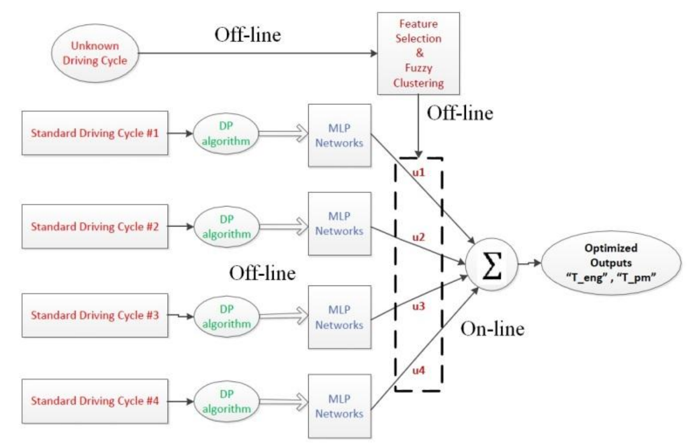

Figure 9 – Structure of the proposed control strategy

As can be seen in this figure, the control strategy consists of some offline portions and also an online one. At first, the similarity weights between the unknown driving cycle and each of the clusters are computed in an offline way. In addition, the optimized control strategies correspond to four standard driving cycles are derived using the DP algorithms. After that, the MLP networks are trained by the results of four DP algorithms. The two latest processes are done in the offline mode, either. The only online portion of the intelligent control strategy is the linear combination of the MLP networks' output. By multiplying the fuzzy similarity weights in the MLP networks' outputs, the final output of the controller is computed:

$$output = \sum_{i=1}^{4} u_i \times MLP_i \tag{9}$$

The optimized value for the torque of the ICE is the output of the intelligent control strategy. The value for the torque of the hydraulic P/M is determined by subtracting the optimized ICE torque from the value of the demand torque.

In order to implement the intelligent control strategy, the MLP networks have been modeled in MATLAB/Simulink. One block of the MLP models is shown in Fig. 10. There are four MLP blocks correspond to each of the standard driving cycles, in this figure. Also, the multiplication of the MLPs' outputs by the fuzzy weights can be seen. It should be noticed that there are 5 blocks like the one shown in Fig. 10 in the model of the intelligent control strategy. Each of these blocks is correspond to each portion of the SOC domain (Fig. 7).

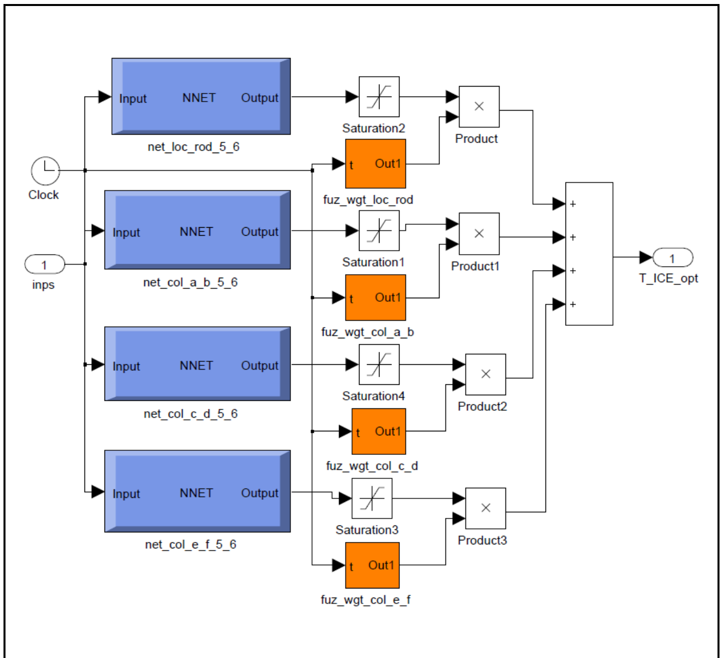

Figure 10 – Corresponding MLP networks for the results of DP algorithms. They are modeled in Simulink

SIMULATION RESULTS

In order to see the utility of the presented intelligent control strategy, the hydraulic hybrid bus model has been simulated by using two different control strategies. One of the simulations has been performed with the proposed intelligent control strategy and the other one has been organized with a rule-based control strategy. There isn't any optimization procedure in the rule-based control strategy. It consists of four distinct modes regarding the regular operation of an urban bus. The torque commands for two power sources are determined by considering some rules. These rules have been defined by the expert knowledge of the designers. So the rule-based control strategy has the same reactions in different driving cycles. That is the main difference between the intelligent control strategy and the rule-based one. The complete explanation of the rule-based control strategy has been proposed by the authors in [12].

The two above simulation cases have been performed for a compound driving cycle. The compound driving cycle contains six distinct portions of the Nuremburg driving cycle. Each of them is 100 seconds long and has been chosen in such a way that the speed at the beginning and also at the end of the cycle would be zero. The compound driving cycle is shown in Fig. 11. Every other arbitrary driving cycle can be used to perform the simulations.

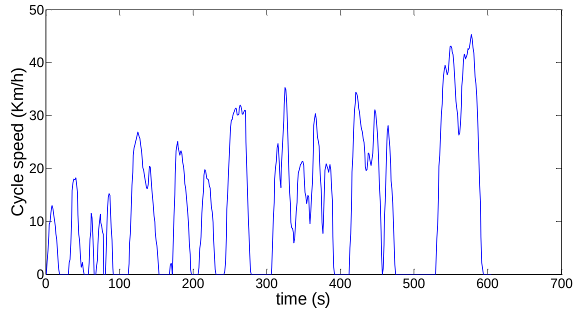

Figure 11 – The compound driving cycle generated using six distinct 100 seconds duration of Nuremburg driving cycle

In order to simulate the PHH bus model with the intelligent control strategy, the similarity weights of the compound driving cycle should be determined. These weights have been evaluated by the feature selection algorithm and the fuzzy c-means clustering which are explained in detail earlier in this paper. Fig. 12 shows the values of the clustering cost function corresponding to the number of features included. It can be seen that only six features are sufficient to reach an acceptable clustering error. In fact, use of more features does not improve performance of the clustering algorithm so much.

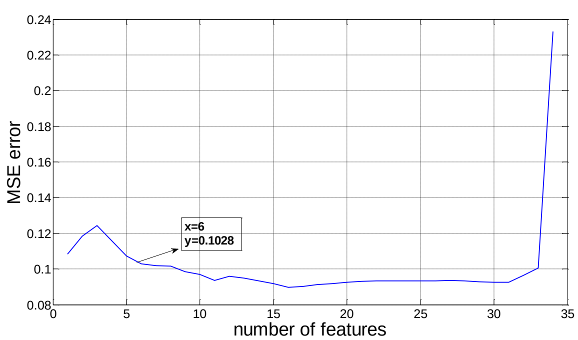

Figure 12 – values of MSE error in fuzzy clustering corresponding to the number of features

Using the six proper features, we adopted weights of similarity between every portion of the compound driving cycle and each of standard driving cycles. The values of these most sufficient features along with the fuzzy weights for every portion of the compound driving cycle are presented in Table 3.

Table 3. The values of six most sufficient features and fuzzy weights for each portion of the compound driving cycle

Parameters	Six distinct 100 seconds duration of Nuremburg driving cycle					
	70 - 170 s	170 - 270 s	270 - 370 s	420 – 520 s	770 – 780 s	920 – 1020 s
Average acceleration (m/s2)	**0.574**	**0.61**	**0.497**	**0.62**	**0.848**	**0.563**
% of time acceleration is between 0.2-0.4 m/s2	**17.65**	**18.52**	**20.00**	**16.28**	**20.00**	**18.75**
Average deceleration (m/s2)	**-0.56**	**-0.36**	**-0.48**	**-0.62**	**-0.56**	**-0.546**
RPA (m/s2)	**0.154**	**0.11**	**0.106**	**0.163**	**0.158**	**0.121**
PKE (m/s2)	**0.75**	**0.79**	**0.677**	**0.96**	**1.28**	**0.831**
% of time production of speed and acceleration is between 5-10 m2/s3	**69.31**	**54.45**	**62.33**	**47.52**	**55.44**	**57.43**
Similarity weight to Arterial/Collector a-b	**0.191**	**0.267**	**0.231**	**0.116**	**0.147**	**0.2233**
Similarity weight to Arterial/Collector c-d	**0.205**	**0.247**	**0.203**	**0.402**	**0.320**	**0.268**
Similarity weight to Arterial/Collector e-f	**0.328**	**0.245**	**0.249**	**0.324**	**0.331**	**0.293**
Similarity weight to Local roadway	**0.277**	**0.241**	**0.318**	**0.158**	**0.202**	**0.216**

After the completion of the two simulation cases, the results using the intelligent control strategy has been compared to the results of simulation using a rule-based one. The comparison between the fuel consumed in each simulation has been shown in Table 4. Also, the values for the error between the cycle speed and the actual bus speed are presented in this table. It should be noticed that the initial and the final SOC of the accumulators in both simulation cases are the same.

Table 4. Comparison of the results of intelligent and rule-based control strategies

Simulation explanation	Total fuel consumption (lit/100km)	MSE error of vehicle speed	% Fuel consumption reduction
rule-based control strategy	**32.983**	**0.0039**	**12.825**
intelligent control strategy	**28.753**	**0.0051**	

In addition, the torque command signals of the ICE for the two simulation cases have been shown in Fig. 13. These signals are presented in short period of time due to show the information more explicitly.

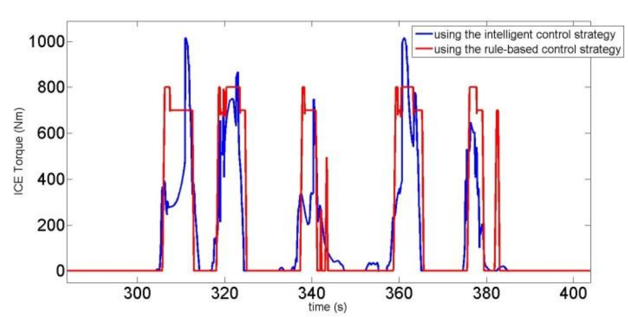

Figure 13 –The torque command signals of the ICE for the simulation cases with intelligent and rule-based control strategies

CONCLUSION

In this study an intelligent control strategy has been designed for a hydraulic hybrid bus. In this control strategy, four standard driving cycles have been chosen as the reference clusters. After that, the optimized control strategies for each of the standard driving cycles have been evaluated by using a dynamic programming algorithm. Then, some MLP networks are trained by the results of the DP algorithms. These networks have been used to determine the proper command signal for an unknown driving cycle. The proposed intelligent control strategy generates the ICE torque command by multiplying the outputs of MLP networks by some weights. These weights define the similarity of every portion of the unknown driving cycle to the four predefined standard driving cycles. The similarity weights are computed by using a feature selection method in conjunction with the fuzzy c-means clustering procedure. Finally, simulations have been performed to see the utility of the intelligent control strategy. According to the simulation results, the PHH bus fuel consumption has been reduced 12.82% by using the proposed intelligent control strategy. The reduction in fuel consumption is in comparison with the results of the simulation using a rule-based control strategy. The reason of fuel consumption reduction can be realized by comparing the torque command signals of the two simulation cases. It can be seen that the portion of the ICE in generation of the driver demand torque is reduced by using the intelligent control strategy. In fact, the use of the ICE torque has been decreased by using the intelligent control strategy. Also, the reduction in fuel consumption has been comprised by an increase in the speed error of the bus. Although the increase of the speed error is equal to 30 percent, the value of the error is still such low that its influence in the performance of the PHH bus can be eliminated.

ACKNOWLEDGMENT

This work was supported by Vehicle, Fuel and Environment Research Institute (VFERI) of University of Tehran.

REFERENCES

[1] Salmasi, F.R., 2007, “Control Strategies for Hybrid Electric Vehicles: Evolution, Classification, Comparison and Future Trend,” IEEE Transaction on vehicular technology, 56(5), pp.2393-2404.
[2] Langari, R. and Won, J.-S., 2005, “Intelligent Energy Management Agent for a Parallel Hybrid Vehicle—Part I: System Architecture and Design of The Driving Situation Identification Process,” IEEE Transaction on vehicular technology, 54(3), pp. 925–934.
[3] Won, J.-S. and Langari, R., 2005, “Intelligent Energy Management Agent for a Parallel Hybrid Vehicle—Part II: Torque Distribution, Charge Sustenance Strategies, and Performance Results,” IEEE Transaction on vehicular technology, 54(3), pp. 935–952.
[4] Abdollahi, A.D., Nikravesh, S.K. and Menhaj, M.B., 2007, “An Intelligent Control Strategy in a Parallel Hybrid Vehicle,” Journal of Iranian Association of Electrical and electronics Engineers, 4(2), pp. 43-52.
[5] Park, J., Chen, Z., Kiliaris, L., Kuang, M.L., Masrur, M.A., Phillips, A.M. and Murphey, Y.L., 2009, “Intelligent Vehicle Power Control Based on Machine Learning of Optimal Control Parameters and Prediction of Road Type and Traffic Congestion,” IEEE Transaction on vehicular technology, 58(9), pp. 4741-4756.
[6] Huang, X., Tan, Y. and He, X., 2009, “An Intelligent Multi-Feature Statistical Approach for the Discrimination of Driving Conditions of a Hybrid Electric Vehicle,” Proc. of international joint Conference on Neural Networks, Atlanta, Georgia, USA, pp. 1286-1293.
[7] Theodoridis, S., Koutroumbas, K., 2006, “*Pattern Recognition*,” third edition, Elsevier, USA, pp. 235-236, Chap. 5, and pp. 600-607, Chap. 14.
[8] Carlson, T.R. and Austin, R.C., 1997, “Development of Speed Correction Cycles,” Sierra Research, Inc., Sacramento, California, Report SR97- 04-01.
[9] PU, J., YIN, C. and ZHANG, J., 2008, “Fuel Optimal Control of Parallel Hybrid Electric Vehicles,” Frontiers of Mechanical Engineering in China, 3(3), pp. 337-342.
[10] Wegleiter, H., Schweighofer, B., Holler, G. and Brunnader, R., 2011, “Fast Quasi Optimal Control Of Hybrid Electric Vehicles Considering Limiting Conditions,” Proc. of EEVC, Brussels, Belgium.
[11] Erricson, E., 2001, “Independent Driving Pattern Factors and Their Influence on Fuel-use and Exhaust Emission Factors,” Transp. Res. Part D, 6(5), pp. 325–341.
[12] Esfahanian, V., Safaie, A. and et. al, 2012,“Design and Modeling of a Parallel Hydraulic Hybrid Bus,” International Conference on Applications and Design in Mechanical Engineering, Penang, Malaysia.